Stabilization of Pores in Lipid Bilayers by Anisotropic Inclusions

Miha Fošnarič,[†] Veronika Kralj-Iglič,[‡] Klemen Bohinc,[†] Aleš Iglič,[†] and Sylvio May*[,§]

Laboratory of Applied Physics, Faculty of Electrical Engineering, University of Ljubljana, Tržaška 25, SI-1000 Ljubljana, Slovenia, Institute of Biophysics, Faculty of Medicine, University of Ljubljana, Lipičeva 2, SI-1000 Ljubljana, Slovenia, and Institute of Molecular Biology, Friedrich-Schiller-University, Winzerlaer Strasse 10, Jena 07745, Germany

Received: April 17, 2003; In Final Form: September 5, 2003

Pores in lipid bilayers are usually not stable; they shrink because of the highly unfavorable line tension of the pore rim. Even in the presence of charged lipids or certain additives such as detergents or isotropic membrane inclusions, membrane pores are generally not expected to be energetically stabilized. We present a theoretical model that predicts the existence of stable pores in a lipid membrane, induced by the presence of anisotropic inclusions. Our model is based on a phenomenological free energy expression that involves three contributions: the energy associated with the line tension of the pore in the absence of inclusions, the electrostatic energy of the pore for charged membranes, and the interaction energy between the inclusions and the host membrane. We show that the optimal pore size is governed by the shape of the anisotropic inclusions: saddle-like inclusions favor small pores, whereas more wedgelike inclusions give rise to larger pore sizes. We discuss possible applications of our model and use it to explain the observed dependency of the pore radius in the membrane of red blood cell ghosts on the ionic strength of the surrounding solution.

Introduction

Biological cells exchange material with the surrounding environment through the cell membrane. One of the mechanisms for transmembrane transport involves the presence of pores in the lipid bilayer, through which a substantial flow of material can take place. For example, pores were observed in red blood cell ghosts,[1−3] where the pore size depends on the ionic strength of the surrounding fluid.[2] The formation of pores in the membrane can also be induced by applying an AC electric field across the membrane.[4] This phenomenon is known as electroporation and has become widely used in medicine and biology.[5−7] Finally, the formation of pores plays an important role in the action of many antimicrobial peptides.[8] A number of theoretical studies have been made to understand the physical basis of electroporation[9,10] and peptide-induced pore formation.[11−14] However, the mechanisms responsible for the energetics and stability of membrane pores are still obscure and require further clarification.

The formation of a pore in a lipid bilayer implies the existence of a bilayer edge. It is likely[15−17] that in the process of pore formation the lipid molecules near the edge of the pore rearrange themselves in such a way that their polar headgroups shield the hydrocarbon tails from water (Figure 1). Modified molecular packing of the phospholipid molecules at the bilayer edge causes the membranes to have high line tension, Λ, that is, high *excess* energy per unit length of the exposed edge, making pores energetically unfavorable. In fact, even if the membrane is subject to a lateral tension, holes in membranes are not stable: they either shrink, or above a critical size, they grow. On the other hand, there are various examples in which membrane pores live long enough to be observed experimentally.[2,18−20] The question arises what mechanisms could be responsible for the stabilization of pores against immediate and spontaneous closure or widening.

One such mechanism has recently been suggested by Betterton and Brenner.[21] It applies to charged membranes and is based on competition between line tension and electrostatic repulsion between the opposed membrane rims within a pore. An analysis based on linearized Poisson−Boltzmann theory showed for certain combinations of membrane charge density, σ, line tension, Λ, and Debye length, l_d, that holes become energetically stabilized. However, for common lipid membranes, the depth of the minimum is so shallow—below kT where k is Boltzmann's constant and T the absolute temperature—that additional stabilizing effects are required to explain the existence of experimentally observed pores.[21]

In the present work, we suggest and analyze a different explanation for the stabilization of pores in fluid membranes, the presence of anisotropic inclusions. Inclusions are rigid, membrane-inserted bodies that appear in biological or model membranes such as (often transmembrane) proteins or peptides, detergents, or sterols. If not all in-plane orientations of the inclusion are energetically equivalent, then the inclusion is referred to as *anisotropic*. Anisotropic inclusions are candidates for the formation of membrane pores because the pore rim provides a lipid packing geometry with which anisotropic inclusions can favorably interact.[22−27] Of particular interest in this respect are certain antimicrobial peptides. These peptides are positively charged and amphipathic, often exhibiting their lytic activity through the cooperative formation of membrane pores.[8,19] Most importantly in connection with the present work, antimicrobial peptides are typically elongated in shape, which renders their interaction with curved membranes highly anisotropic. Examples of anisotropic inclusions also include various lipids[28] (certain cationic lipids,[29] glycolipids, or lipoproteins[30]),

* Corresponding author. E-mail: may@lily.molebio.uni-jena.de. Phone: ++49-3641-657582. Fax: ++49-3641-657520.
[†] Faculty of Electrical Engineering, University of Ljubljana.
[‡] Faculty of Medicine, University of Ljubljana.
[§] Friedrich-Schiller-University.

10.1021/jp035035a CCC: $25.00
Published on Web 10/16/2003

gemini detergents,[31] or detergents with a large and anisotropic headgroup.[32]

The abundance of proteins in biological membranes has motivated numerous theoretical studies on membrane−inclusion interactions; see, for example, the reviews by Gil et al.[33] and Goulian[34] and references therein. Among the various lines of research, some focus has recently been put on *anisotropic* inclusions. These inclusions are nonaxisymmetric but, for simplicity, are usually considered to still have quadrupolar symmetry. One principal question concerns the lateral organization of anisotropic inclusions and the corresponding response of the membrane shape. This question was addressed recently on two different levels of approximation.

The first approach considers *individual* inclusions. Here, an angular matching condition between a given inclusion and the host membrane is imposed. For example, a single isotropic inclusion induces a catenoid-like membrane shape (for which the mean curvature vanishes at each given point). Interference of the inclusion-induced membrane perturbations gives rise to membrane-mediated interaction between inclusions. For two isotropic inclusions, this interaction is known to be repulsive, at least in the low-temperature limit.[35] However, more than two inclusions (isotropic or anisotropic) cause nontrivial many-body effects that induce complex spatial patterns of the inclusion arrangement.[36−38]

There is a second, mean-field level approach[27] which we adopt in the present work. Here, a given small membrane patch contains an ensemble of inclusions. The inclusions do not individually deform the membrane but energetically couple to the shape of the membrane patch. Note that the shape of the membrane patch is prescribed (but may later be optimized). The coupling between the inclusions and the membrane results from a mismatch of the given membrane curvatures and the preferred ("spontaneous") curvatures of the inclusions. Thus, the membrane curvatures act as a mean-field that must self-consistently be determined so as to minimize the overall free energy, yielding the local inclusion density everywhere on the membrane and the corresponding optimal membrane shape.

We will show that anisotropic membrane inclusions are candidates for the stabilization of pores in lipid bilayers. To this end, we analyze the energetics of a single membrane pore in a binary lipid membrane, consisting of (charged) lipids and anisotropic inclusions. The free energy of the inclusion-doped membrane contains the line tension contribution due to the rearrangement of lipids within the pore region, the interaction energy between the anisotropic inclusions and the membrane, and the electrostatic energy of the charged lipids. The latter is taken into account to allow a prediction of how the pore size depends on the salt concentration.

Theoretical Model

We consider a lipid membrane that contains a single pore. For our purpose, it is most convenient to assume a perfectly planar membrane and a pore of circular shape, say of aperture radius r. We locate a Cartesian coordinate system at the pore center with the axis of rotational symmetry (the z-axis) pointing normal to the bilayer midplane. The presence of the membrane pore is likely to imply some structural rearrangement of the lipids at the bilayer rim. This reorganization is driven by the unfavorable interaction of the lipid tails when exposed directly to the aqueous environment. Even though experimentally obtained evidence is currently not available, it seems a reasonable approximation to assume (and we base our present work on this notion) that the lipids within the rim assemble into a semitoroidal cap to shield the hydrocarbon chains from contact with the aqueous environment. The height of the cap fits the bilayer thickness $2b$, implying a radius, b, of its circular cross-sectional shape. The pore geometry is schematically shown in Figure 1. A parametrization of the semitoroidal cap is given by $x = b\cos\varphi\,(r/b + 1 + \cos\theta)$, $y = b\sin\varphi\,(r/b + 1 + \cos\theta)$, and $z = b\sin\theta$ with $0 \le \varphi \le 2\pi$ and $\pi/2 \le \theta \le 3\pi/2$. The principal curvatures of the cap are then

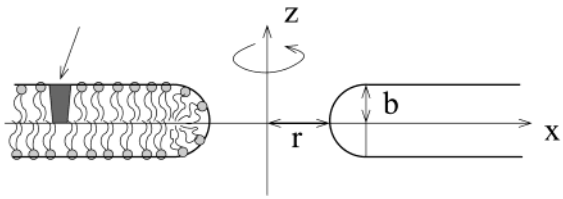

Figure 1. A planar lipid bilayer with a pore in the center. The figure shows the cross-section in the $x-z$ plane. Rotational symmetry around the z-axis is indicated. On the left side, the packing of the lipid molecules is shown schematically. The headgroups of lipid molecules are represented by filled circles. The arrow denotes the membrane inclusion, which is shown schematically.

$$C_1 = \frac{1}{b} \qquad C_2 = \frac{\cos\theta}{r + b(1 + \cos\theta)} \tag{1}$$

and the area element $\mathrm{d}A_P = b[r + b(1 + \cos\theta)]\,\mathrm{d}\varphi\,\mathrm{d}\theta$. The local geometry within the rim is saddle-like everywhere and most pronounced at $\theta = \pi$ where $C_1/C_2 = -r/b$. Note again that the semitoroidal shape of the rim is an assumption; alternative choices could be considered but are not expected to alter the conclusions of the present work.

Our objective is to analyze the influence of anisotropic inclusions on the energetics of a membrane pore. As is well-known, lipid membranes are two-dimensional fluids that allow inserted inclusions to redistribute laterally. Consequently, inclusions accumulate at energetically beneficial membrane regions or even induce their formation. The creation of a membrane pore is a drastic example for an inclusion-induced reorganization of a lipid membrane. Obviously, if inclusions induce stable pores, they must be able to affect substantially the pore free energy F as a function of the pore radius r.

To obtain the equilibrium size of the pore, the overall free energy, F, of the pore is minimized. We assume that F is the sum of three contributions:

$$F = W_{\mathrm{edge}} + U_{\mathrm{el}} + F_{\mathrm{i}} \tag{2}$$

where W_{edge} is the energy due to the line tension of a lipid bilayer without the inclusions, U_{el} is the electrostatic energy of the charged lipids, and F_{i} is the energy due to the interactions between the membrane inclusions and the host membrane. We note that F and all its contributions are *excess* free energies, measured with respect to a planar, pore-free membrane. We also note that our work does not involve any additional constraints of the membrane area, A. Hence, we work at vanishing lateral tension, as should be appropriate for most bilayers.

Line Tension of a Lipid Bilayer. The modified molecular packing of the lipid molecules at the edge of the pore (see Figure 1) entails an energy cost W_{edge}. For an inclusion-free membrane, this energy cost is given by $W_{\mathrm{edge}} = 2\pi\Lambda r$, where r is the radius of the circular membrane pore and Λ is the line tension (i.e., energy per unit length of the exposed edge) of the lipid bilayer. One can easily obtain a rough estimate for Λ on the basis of the elastic energy required to bend a lipid monolayer into a semicylindrical micellar cap. Adopting the usual quadratic

curvature expansion for the free energy according to Helfrich,[39] one finds[16] $\Lambda = \pi k_c/(2b)$ where k_c is the lipid layer's bending rigidity. Typically for a single lipid layer, $b = 2.5$ nm and $k_c = 10kT$, implying $\Lambda \approx 6kT/\text{nm} \approx 2 \times 10^{-11}$ J/m (at room temperature). Indeed, this order of magnitude corresponds to experimental results for the line tension of lipid bilayers.[18,40,41] It is worth noting that the semicylindrical micellar cap has large curvatures, $C_1 = 1/b$ and $|C_2| \leq 1/r$, for which the quadratic curvature expansion might completely fail.[18] The fact that it does not fail indicates the robustness of the membrane elasticity approach; it is often used successfully to model experimentally observed structural reorganization of lipid assemblies, even if that involves large changes in curvature.[42,43]

If rigid membrane inclusions are present within the membrane pore, they replace some of the lipids, depending on their lateral extensions. The replaced lipids no longer contribute to the line tension W_{edge}. We shall account approximately for this reduction in line tension by writing

$$W_{edge} = 2\Lambda(\pi r - N_P R_i) \tag{3}$$

where N_P denotes the number of inclusions within the membrane rim and $2R_i$ is the lateral extension of the cross-sectional shape of the inclusions. Steric interactions limit the number of inclusions within the membrane rim; $N_P \leq N_P^{max} = \pi r/R_i$. Thus $W_{edge} \geq 0$, and the line tension always provides a tendency for the pore to shrink.

Electrostatic Energy of a Pore. The calculation of the electrostatic energy of a membrane pore follows Betterton and Brenner[21] who derived an expression valid for a very thin membrane ($b \rightarrow 0$) in linearized Poisson−Boltzmann (PB) theory. It is well-known that linearized PB theory greatly overestimates the electrostatic free energies for lipid membranes. Yet, solutions within nonlinear Poisson−Boltzmann theory (and for more realistic choices of b) are numerically demanding. Hence, to keep our model tractable, we adopt the result of linear PB theory where the equation $\nabla^2\phi = \kappa_d^2\phi$ determines the (dimensionless) electrostatic potential, ϕ, at a given Debye length $l_d = \kappa_d^{-1} = \sqrt{\epsilon_w\epsilon_0 kT/(2n_0 N_A e_0^2)}$. Here ϵ_w is the dielectric constant of the aqueous solution, ϵ_0 is the permittivity of free space, n_0 is the ionic strength of the surrounding solution (i.e., bulk salt concentration, assuming a 1:1 salt such as NaCl), N_A is Avogadro's number, and e_0 is the unit charge.

The solution of the linear PB equation is written as the difference, $\phi(x,z) = \phi_\infty(z) - \phi_0(x,z)$, between the electrostatic potential of a flat infinite pore-free membrane (ϕ_∞) and the electrostatic potential of the circular flat membrane segment with radius r (ϕ_0), both having constant surface charge density, σ. The value of ϕ_∞ is[44] $\phi_\infty(z) = (\sigma/(\epsilon_w\epsilon_0\kappa_d))\exp(-\kappa_d z)$. The expressions for ϕ_0 can be obtained using the Hankel transformation and taking into account the boundary conditions $\phi(z\rightarrow\infty) = 0$ and $\partial_z\phi(z=0) = 0$ for $x > r$, $\partial_z\phi(z=0) = -\sigma/(\epsilon_w\epsilon_0)$ for $x < r$. Then the electric potential $\phi(x,z)$ can be written as

$$\phi(x,z) = +\frac{\sigma}{\epsilon_w\epsilon_0\kappa_d} e^{-\kappa_d z} - \frac{\sigma r}{\epsilon_w\epsilon_0}\int_0^\infty \frac{J_0(kx)J_1(kr)}{\sqrt{\kappa_d^2 + k^2}} e^{-z(\kappa_d^2+k^2)^{1/2}}\,dk \tag{4}$$

where J_0 and J_1 are Bessel functions.

Using eq 4 for the electric potential, we can derive the electrostatic free energy via a charging process:[44,45]

$$U_{el,tot} = 2\pi\int_0^\infty \sigma(x)\phi(z=0)x\,dx \tag{5}$$

Equation 5 can be further processed analytically. By subtracting the electrostatic energy of the charged pore-free membrane, one obtains an explicit expression for the *excess* electrostatic energy of the pore:

$$U_{el} = -\frac{\pi\sigma^2 r^2}{\epsilon_w\epsilon_0\kappa_d} + \frac{2\pi\sigma^2 r^3}{\epsilon_w\epsilon_0}\int_0^\infty \frac{J_1(x)^2}{x\sqrt{x^2 + \kappa_d^2 r^2}}\,dx \tag{6}$$

This is the result of Betterton and Brenner,[21] which we shall use in our present work.

Free Energy of Inclusions. Membrane inclusions are embedded within the host membrane, and the inclusion−membrane interactions are mainly governed by the hydrophobic effect. To describe the corresponding free energy, F_i, we use a phenomenological model[26] in which the mismatch between the effective intrinsic shape of the inclusions and the actual shape of the membrane at the site of the inclusions causes an interaction energy. The actual shape of the membrane at the site of the inclusion can be described by the diagonalized curvature tensor $\mathbf{C}$,

$$\mathbf{C} = \begin{bmatrix} C_1 & 0 \\ 0 & C_2 \end{bmatrix} \tag{7}$$

where C_1 and C_2 are the two principal curvatures. Similarly, the intrinsic shape of a given inclusion can be described by the diagonalized curvature tensor $\mathbf{C}_m$,

$$\mathbf{C}_m = \begin{bmatrix} C_{1m} & 0 \\ 0 & C_{2m} \end{bmatrix} \tag{8}$$

where C_{1m} and C_{2m} are the two intrinsic principal curvatures of the inclusion. In general, inclusions are anisotropic,[22,23,27,28,31] which means that $C_{1m} \neq C_{2m}$. The principal directions of the tensor $\mathbf{C}$ deviate in general from the principal directions of the tensor $\mathbf{C}_m$; say, a certain angle ω quantifies this mutual rotation. The single-inclusion energy (E_i) can then be expressed in terms of the two invariants (trace and determinant) of the mismatch tensor $\mathbf{M} = \mathbf{R}\mathbf{C}_m\mathbf{R}^{-1} - \mathbf{C}$ where $\mathbf{R}$ is the rotation matrix,

$$\mathbf{R} = \begin{bmatrix} \cos\omega & -\sin\omega \\ \sin\omega & \cos\omega \end{bmatrix} \tag{9}$$

Terms up to second order in the elements of the tensor $\mathbf{M}$ are taken into account:

$$E_i = \frac{K}{2}(\text{tr}\,\mathbf{M})^2 + \bar{K}\det\mathbf{M} \tag{10}$$

where K and $\bar{K}$ are the interaction constants between the inclusion and the surrounding membrane. Using eqs 7−10, we can write the single-inclusion energy (E_i) in the form[27]

$$E_i = (2K + \bar{K})(H - H_m)^2 - \bar{K}[D^2 - 2DD_m\cos(2\omega) + D_m^2] \tag{11}$$

Quantities $H = (C_1 + C_2)/2$ and $H_m = (C_{1m} + C_{2m})/2$ are the respective mean curvatures, while $D = (C_1 - C_2)/2$ and $D_m = (C_{1m} - C_{2m})/2$ are the curvature deviators. Curvature deviator D_m describes the intrinsic anisotropy of the single membrane inclusion.[26,28]

The time scale for orientational changes of the anisotropic inclusions is usually small compared to shape changes of the lipid bilayer. It is therefore reasonable to employ an orientational averaging of the inclusions according to the rules of statistical

mechanics. To this end, we take into account that the inclusions can rotate around the axis defined by normal to the membrane at the site of the inclusion. Then the partition function, q, of a single inclusion is[22,28]

$$q = \frac{1}{\omega_0}\int_0^{2\pi} \exp\left(-\frac{E_i(\omega)}{kT}\right) d\omega \qquad (12)$$

where ω_0 is an arbitrary angle quantum. Inclusions can also move laterally over the phospholipid layer, so they can distribute laterally over the membrane in the way that is energetically the most favorable.[23,27] The lateral distribution of the inclusions in a membrane of overall area A is in general nonuniform. Treating inclusions as pointlike, independent, and indistinguishable, we can derive the expression for the contribution of the inclusions to the membrane free energy on the basis of eqs 11 and 12:[27]

$$\frac{F_i}{kT} = -N \ln\left[\frac{1}{A}\int_A q_c I_0\left(\frac{2\bar{K}}{kT}DD_m\right) dA\right] \qquad (13)$$

where N is the total number of inclusions in the membrane, q_c is defined as

$$q_c = \exp\left(-\frac{2K+\bar{K}}{kT}(H^2 - 2HH_m) + \frac{\bar{K}}{kT}D^2\right) \qquad (14)$$

and I_0 is the modified Bessel function. The integration in eq 13 is performed over the whole area, A, of the membrane, including the pore region of area A_P and the two flat monolayers that constitute the planar bilayer part. Recall that F_i in eq 13 (together with eq 14) is an *excess* free energy with respect to the pore-free planar membrane, as was defined in eq 2. Indeed, it is $F_i(H=D=0) = 0$ and hence only those inclusions that are located within the pore rim (but not those in the planar membrane) contribute to F_i. Because the overall area A is assumed to be large, we can expand F_i with respect to A, yielding

$$\frac{F_i}{kT} = n\int_{A_P}\left[1 - q_c I_0\left(\frac{2\bar{K}}{kT}DD_m\right)\right] dA_P \qquad (15)$$

where $n = N/A$ is the area density of the inclusions in the membrane and where the integration extends only over the area, A_P, of the membrane rim. The influence of the inclusion's anisotropy is contained in the Bessel function $I_0(2DD_m\bar{K}/(kT))$ (the coefficient q_c is independent of D_m). Because $I_0 \geq 1$, we see from eq 15 that the anisotropy of inclusions always tends to lower F_i. Yet, whether inclusions eventually lower or increase F depends on all inclusion properties, on the geometry (D_m and H_m) and on the interaction constants (K and $\bar{K}$).

We also note that the number of inclusions contained within the membrane rim is given by

$$N_P = n\int_{A_P} q_c I_0\left(\frac{2\bar{K}}{kT}DD_m\right) dA_P \qquad (16)$$

Combination of eqs 15 and 16 yields

$$\frac{F_i}{kT} = nA_P - N_P \qquad (17)$$

Of course, if no energetic preference exists for the inclusions to partition into the membrane rim ($q_c I_0 = 1$), then eq 16 predicts $N_P/A_P = n$ and thus $F_i = 0$. On the other hand, if the density of the inclusions within the pore region greatly exceeds the bulk density, then $nA_P \ll N_P$ and $F_i \approx -N_P kT$. Hence, each inclusion that enters the membrane pore in excess to the bulk density contributes $1kT$ to the inclusion free energy. The inclusion size determines the maximal number, N_P^{max}, that can enter the pore rim. For rather large inclusions $R_i \approx b$ and small pores $r \approx b$, we expect that N_P^{max} is of the order of a very few inclusions. That seems to indicate that for small pores F_i is not able to decrease F by more than a few kT. Below we show that nevertheless, for charged membranes, anisotropic inclusions can dramatically reduce F (substantially more than $-N_P kT$).

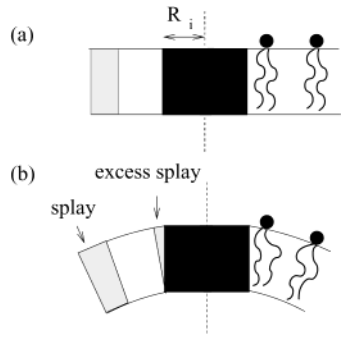

Figure 2. Cross sections through a lipid layer containing a single cylindrical inclusion (black square). Some lipids are shown schematically. In the planar layer (a), all lipids pack, on average, into a cylindrical shape (schematized by the shaded rectangle). Bending the monolayer (b) induces a splay deformation of the lipids. Because the inclusion is rigid, it cannot participate in the splay deformation, thus inducing an extra (excess) splay of the lipids in its vicinity.

Estimation of the Constants. We discuss a simple generic, molecular-level model for the interaction between a single anisotropic inclusion and a lipid bilayer of principal curvatures C_1 and C_2 into which the inclusion is embedded. The model allows us to estimate the phenomenological constants, K, $\bar{K}$, H_m, and D_m, in terms of the inclusion shape and the elastic properties of the lipid bilayer.

Bending a lipid layer implies a change in the average molecular shape of each individual lipid: a splay (or saddle-splay) deformation is imposed by the membrane curvature. Membrane-embedded inclusions cannot participate in the curvature-induced splay deformation because of their stiffness. That is, some lipids in the vicinity of the inclusion have to compensate for the stiffness of the inclusion by adopting an additional ("excess") splay, beyond that of the lipids far from the inclusion. Figure 2 provides a schematic illustration of this mechanism for a cylindrical inclusion of radius R_i. The energy associated with the excess splay determines the inclusion energy F_i. It depends on both the inclusion's shape and size and the elastic properties of the lipid layer.

The inclusion's shape can conveniently be characterized by a circular cross section (of radius R_i) and a modulated "cone angle" $\theta_i(\phi) = \bar{\theta}_i + \Delta\theta_i \cos(2\phi)$ along its circumference with a corresponding azimuthal angle ϕ. The average "coneness" of such an inclusion is $\bar{\theta}_i$, and the deviation along the inclusion's circumference is $\Delta\theta_i$. Clearly, for $\Delta\theta_i = 0$, the inclusion is isotropic, and for $\Delta\theta_i = \bar{\theta}_i = 0$, the inclusion is cylindrical.

The elastic properties of a lipid layer can be characterized by the bending constant k_c and the area stretching modulus K_c. From membrane elasticity theory, it is well-known[46,47] that the decay length of the perturbation induced by a single inclusion is $\xi = \sqrt{2}b(k_c/(K_c b^2))^{1/4}$. If the inclusion radius is not much smaller than ξ (that is, for $R_i \gtrsim \xi$), one can roughly estimate

the interaction constants

$$K \approx \frac{3}{2}\pi k_c \frac{R_i^3}{\xi}, \qquad \bar{K} \approx -\frac{2}{3}K \tag{18}$$

as well as

$$H_m = \frac{\bar{\theta}_i}{R_i}, \qquad D_m = \frac{\Delta\theta_i}{R_i} \tag{19}$$

The derivation of eqs 18 and 19 will be given elsewhere. Note that the interaction constants K and $\bar{K}$ depend not only on the monolayer's bending stiffness k_c but also on the area stretching modulus K_c (through ξ). The presence of K_c implies that local changes in the thickness of the monolayer leaflets are involved in the spatial relaxation of the inclusion-induced perturbation. This is not obvious because we do not impose any thickness mismatch between the inclusion and the membrane. However, as Figure 2 illustrates, insertion of the inclusion imposes an angular mismatch which spatially relaxes with the same decay length as a thickness mismatch.[47−49] The relaxation involves a compromise between splay and dilation of the lipid chains.

Typically for a lipid layer $\xi = 1$ nm, $k_c = 10kT$, and thus $K \approx 50R_i^3kT$/nm and $\bar{K} \approx -33R_i^3kT$/nm. The interaction constants increase strongly with the inclusion radius R_i. Because the validity of eq 18 requires $R_i \gtrsim 1$ nm (below we shall use $R_i = b/2 = 1.25$ nm), our present estimate will necessarily predict a strong membrane−inclusion interaction. To this end, we note that eq 11 with $D_m = 0$ has the same structure as the Helfrich bending energy for isotropic membranes. The corresponding interaction constant, K, (and similarly for $\bar{K}$) for a lipid membrane could thus be identified[28] with $K = k_c a_0$, where $k_c \approx 10kT$ is the bending constant of an ordinary lipid monolayer (that is part of a bilayer membrane) and $a_0 = 0.6-0.8$ nm^2 is the cross sectional area per lipid. Thus $k_c a_0 \approx 7kT$ nm^2, which is at least an order of magnitude smaller than the interaction constant K in eq 18. Hence, sufficiently large, rigid membrane inclusions are generally expected to partition strongly into "appropriately curved" membrane regions.

We note that partitioning rigid inclusions into the rim of a membrane pore—besides causing an extra (*excess*) splay, see above—also replaces some structurally perturbed lipids. These lipids no longer contribute to the energy of the pore. The corresponding energy gain is not contained in F_i because we have taken it into account already in W_{edge} (see eq 3).

Results and Discussion

All of the following results are derived for a fixed thickness, $b = 2.5$ nm, of the lipid layer, for a line tension of $\Lambda = 10^{-11}$ J/m, and for a surface charge density $\sigma = -0.05$ A s/m^2 $= -e_0/3.2$ nm^2 of the lipid layer. Taking into account a typical cross-sectional area per lipid of $a_0 = 0.6-0.8$ nm^2, the value for σ would correspond roughly to a 1:4 mixture of (monovalently) charged and uncharged lipids. This is not an unusual situation in (biological and model) membranes.

Inclusion-Free Membrane. Let us start with an inclusion-free membrane. This case has recently been analyzed by Betterton and Brenner.[21] The free energy consists only of the line tension contribution (see eq 3) and the electrostatic free energy (see eq 6); the former favors shrinking and the latter growing of a membrane pore. The parameter that governs the resulting behavior is the Debye length, l_d. For small l_d, pores close; for large l_d, pores grow. Betterton and Brenner have found that for intermediate l_d a local minimum in $F(r)$ exists that may give rise to stable pores. As an illustration, we plot $F(r)$ in Figure 3 for three different choices of l_d, namely, $l_d =$ (a) 2.6, (b) 2.8, and (c) 3.0 nm; a local minimum in $F(r)$ is present only in curve b. Figure 3 exemplifies a general finding: the local minimum of $F(r)$ is very shallow—below kT—and appears in a very narrow region of l_d. Hence, pores in lipid membranes cannot be stabilized solely by electrostatic interactions. Whether the local minimum in $F(r)$ will be preserved in a full nonlinear PB treatment is not known to us.

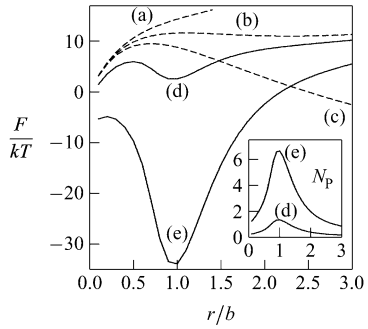

Figure 3. The pore free energy, F, as a function of the pore size, r. The dashed lines correspond to a charged inclusion-free membrane of charge density $\sigma = -0.05$ A s/m^2 with Debye length $l_d =$ (a) 2.6, (b) 2.8, and (c) 3.0 nm. The solid lines describe the effect of adding anisotropic inclusions (characterized by $K = 98kT$ nm^2, $\bar{K} = -2K/3$, $C_{1m} = -C_{2m} = 1/b$) to the charged membrane with $\sigma = -0.05$ A s/m^2 and $l_d = 2.8$ nm. The inclusion concentrations are (d) $n = 1/70\,000$ nm^2 and (e) $n = 1/14\,000$ nm^2. The inset shows the corresponding numbers N_P as function of b/r for curves d and e.

Saddle-Shaped Inclusion. Let us now add anisotropic inclusions to the charged membrane. As argued above, we shall employ the interaction constants $K \approx 50R_i^3kT$/nm and $\bar{K} = -2K/3$. The inclusion radius R_i should be larger than $\xi \approx 1$ nm; we shall use $R_i = b/2 = 1.25$ nm. To illustrate the effect of the inclusion's anisotropy, we chose a perfectly saddle-like inclusion with $C_{1m} = -C_{2m} = 1/b$. Figure 3 shows $F(r)$ for two examples of different area density, n, of the inclusions: $n = 1/70\,000$ nm^2 (curve d), and $n = 1/14\,000$ nm^2 (curve e). We clearly see the pronounced ability of the inclusions to lower and deepen the local minimum of $F(r)$. Because of their favorable interaction, the anisotropic inclusions tend to accumulate within the membrane rim. The corresponding number, N_P, of inclusions in this region is given in eq 16. This number is plotted in the inset of Figure 3 for $n = 1/70\,000$ nm^2 (curve d) and $n = 1/14\,000$ nm^2 (curve e). Recall that the statistical mechanical approach leading to eq 15 is based on pointlike particles. Within this approach, the inclusion size will not limit entry into the pore rim. Yet, for a realistic (that is, nonvanishing) size (recall our choice $R_i = b/2$), N_P should stay sufficiently small to ensure steric fitting of the inclusions into the pore. In fact, at $r = b$, there is full coverage for $N_P = N_P^{max} = \pi b/R_i = 2\pi$. More precisely, the interactions of the inclusions with the membrane rim should dominate over direct inclusion−inclusion interactions. For the examples shown in Figure 3, the inclusion number, N_P, is not prohibitively high. But above $n = 1/14\,000$ nm^2, our present approach (with the present choice of interaction parameters, particularly with $C_{1m} = -C_{2m} = 1/b$), is no longer applicable.

The minimum for $n = 1/14\,000$ nm^2 (curve e in Figure 3) is roughly $F = -30kT$. It arises from the presence of inclusions in the pore region. On the other hand, eq 17 predicts that the inclusion energy $F_i \approx -N_P kT$. The inset of Figure 3 shows that $N_P \leq 6$. Hence, the deep minimum of F does not arise solely from the inclusion contribution F_i. It is also the electrostatic

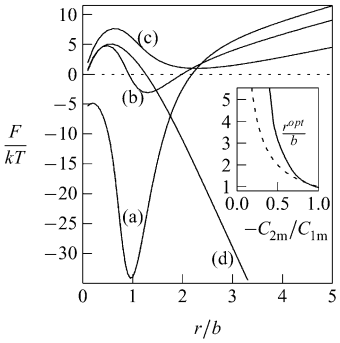

Figure 4. The pore free energy, F, as a function of the pore size, r, for differently shaped anisotropic inclusions: C_{2m}/C_{1m} = (a) −1, (b) −0.8, (c) −0.6, and (d) 0. In all cases, the membrane is charged (σ = −0.05 A s/m^2, l_d = 2.8 nm), and it is $C_{1m} = 1/b$ and n = 1/14 000 nm^2. The inset shows the position of the local minima, r^{opt}, as a function of C_{2m}/C_{1m} (solid line). The dashed line in the inset shows $-C_{2m}/C_{1m} = b/r^{opt}$.

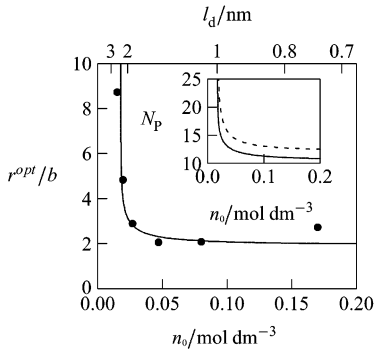

Figure 5. The optimal pore size r as a function of the ionic strength of the surrounding aqueous medium. The charge density of the membrane is σ = −0.05 A s/m^2, the area density of the inclusions is n = 1/2000 nm^2, and the inclusion's preferred curvatures are $C_{1m} = 1/b$ and C_{2m}/C_{1m} = −0.4. Experimental values[2] are also shown (●). The inset shows the actual number of inclusions, N_P, residing in the pore of optimal size, r^{opt} (solid line), and the maximal number, $N_P^{max} = \pi r^{opt}/R_i$ (broken line).

energy, U_{el}, which lowers F. To explain the mechanism, we recall that in the inclusion-free membrane the electrostatic energy and the line tension nearly balance each other. If inclusions enter the pore region, they reduce the line tension (see eq 3). As a result, U_{el} is no longer counterbalanced by W_{edge} and thus strongly lowers F. It can be therefore concluded that also in the case of the charged membranes the deepness of the minimum of F is mainly determined by the inclusions, directly because of their energy contribution F_i and indirectly because of their influence on $U_{el} + W_{edge}$.

Influence of Inclusion Shape. Deepening of the minimum in $F(r)$ occurs in Figure 3 at $r \approx b$ [see curves d and e]. This reflects our choice of the inclusion geometry, $C_{1m} = -C_{2m} = 1/b$. In fact, for $r = b$, the principal curvatures of the rim at $\theta = \pi$ (see eq 1) are $C_1 = -C_2 = 1/b$, coinciding with the inclusion's preference. This observation suggests the possibility of increasing the optimal size of the pore by altering the intrinsic curvatures of the inclusion from a saddle-like ($C_{2m}/C_{1m} \approx -1$) toward a more wedgelike shape ($C_{2m}/C_{1m} \approx 0$). The smaller the magnitude of $|C_{2m}/C_{1m}|$, the larger should be the preferred pore size. With regard to the principal curvatures at the waist of the rim, $C_1 = 1/b$ and $C_2 = -1/r$, one would expect the optimal pore size, r^{opt}, to be determined by the relation

$$-\frac{C_{2m}}{C_{1m}} = -\frac{C_2}{C_1} = \frac{b}{r^{opt}} \qquad (20)$$

In Figure 4, we add anisotropic inclusions of area density n = 1/14 000 nm^2 to a charged membrane (σ = − 0.05 A s/m^2, l_d = 2.8 nm); the shape of the inclusions is characterized by $C_{1m} = 1/b$ and (a) $C_{2m}/C_{1m} = -1$, (b) $C_{2m}/C_{1m} = -0.8$, (c) $C_{2m}/C_{1m} = -0.6$, and (d) $C_{2m}/C_{1m} = 0$. Indeed, the local minimum of $F(r)$ shifts to larger pore sizes as the inclusions become more wedge-shaped [compare the position of the local minimum of curves a−c]. The solid line in the inset of Figure 4 shows how the optimal pore radius r^{opt} changes with C_{2m}/C_{1m}. The broken line in the inset displays the prediction according to eq 20. Clearly, the optimal pore size, r^{opt}, is even larger than what would be expected from the inclusion's geometry. The reason can be found in the presence of the inclusion reservoir in the bulk membrane. Increasing the pore size allows incorporation of more inclusions that interact only somewhat less favorably with the membrane rim.

Our calculations also show that below a critical ratio of $|C_{2m}/C_{1m}|$ the local minimum in $F(r)$ vanishes (in Figure 4, we find $|C_{2m}/C_{1m}| < 0.4$), and the pore grows. Again, the inclusion reservoir in the membrane favors additional partitioning into the membrane rim, which increases the pore size. Below a critical ratio of $|C_{2m}/C_{1m}|$, this process never stops. We also note that for *isotropic* inclusions (where $C_{1m} = C_{2m}$), we do not find energetically stabilized pores. Even more generally, if C_{1m} and C_{2m} have the same sign, stable pores cannot be predicted. Stabilization of the pore derives from the matching of the rim geometry with the inclusion's preference. The rim provides a saddle-like geometry (that is, different signs of C_1 and C_2); consequently, a saddle-like inclusion geometry (that is, different signs of C_{1m} and C_{2m}) is needed to stabilize a pore.

Salt Concentration and Pore Size. In all of the examples presented so far, we added anisotropic inclusions to charged membranes with a specifically selected Debye length, l_d = 2.8 nm. We recall from Figure 3 that this was the choice for which an inclusion-free membrane already exhibits a (shallow) minimum in $F(r)$. The question arises whether pores can also be stabilized for uncharged membranes or, more generally, under varying electrostatic conditions. In this respect, it is interesting to note the experimental observation of stable pores in red blood ghosts for which data exist[2] on the optimal pore radius, $r^{opt}(n_0)$, as a function of the salt concentration, n_0. Our present theoretical approach is able to reproduce the experimental data as shown in Figure 5. We used a charge density of σ = −0.05 A s/m^2, an area density of the inclusions of n = 1/2000 nm^2, and an inclusion geometry characterized by $C_{1m} = 1/b$ and C_{2m}/C_{1m} = −0.4. The inset of Figure 5 shows the corresponding number of inclusions (solid line), as well as the maximal number $N_P^{max} = \pi r^{opt}/R_i$ (broken line) at which the inclusions would sterically occupy the entire rim. The observation $N_P < N_P^{max}$ indicates the applicability of our approach for the selected area density (n = 1/2000 nm^2). Of course, the number of approximations in our approach may still render the good agreement in Figure 5 fortuitous. What adds to this uncertainty is the complexity of the red blood cell membrane. In particular, the attached cytoskeleton can be expected to affect the membrane pore energetics. Therefore, Figure 5 should be understood as an illustration of the principal ability of anisotropic membrane inclusions to stabilize membrane pores, even under changing electrostatic conditions.

In our present investigation, we included electrostatic interactions to allow a prediction of how the pore size depends on salt content. Note that it is generally the anisotropy of the inclusions but not electrostatic interactions that stabilizes pores. Thus, for

uncharged membranes or in the limit of high salt content, qualitatively similar considerations as those presented above account for pore stability. However, the minimum of the overall free energy F would be less deep compared to the case of charged membranes.

Isotropic vs Anisotropic Inclusions. The influence that admixed inclusions have on the energetics (particularly the line tension) of membrane pores is often interpreted in terms of altering the elastic properties of the membrane. For example, the addition of cosurfactants typically reduces the bending stiffness of a membrane.[50] Even more important for membrane pores, the presence of conelike (and analogously, inverted conelike) inclusions can induce a shift in the spontaneous curvature. This shift can be translated into a change in line tension, which provides a common basis for analyzing the energetics of a membrane pore.[18] Our present approach contains this scenario as a special case, namely, if the inclusions are isotropic ($D_m = 0$). In fact, it is the spontaneous mean curvature, H_m, that plays the role of the spontaneous curvature. Beyond the effect of conelike and inverted conelike inclusions, our present approach also allows us to analyze other inclusion shapes, such as wedgelike or saddle-like inclusions. These inclusions can be characterized by an appropriate combination of H_m and D_m. In the following, we shortly discuss a few examples in which we think that the anisotropy of admixed inclusions could be particularly relevant to the pore energetics.

Electroporation is a method of artificial formation of pores in biological membranes by applying an electric field across the membrane. A problem in the electroporation of living tissue is that it often causes irreversible damage to the exposed cells and tissue.[6] Increasing the amplitude of the electric field in electroporation diminishes cell survival rates.[7] On the other hand, if the applied electric field is too low, stable pores are not formed. A way to improve the efficacy of electroporation is chemical modification of the membranes. It has been reported recently[51,52] that adding the nonionic surfactant octaethyleneglycol dodecyl ether ($C_{12}E_8$) to the outer solution of the phospholipid membrane or the cell membrane causes a decrease in the threshold for irreversible electroporation. In other words, $C_{12}E_8$ molecules make transient pores in a membrane more stable. $C_{12}E_8$ molecules were recently suggested to act as anisotropic inclusions in bilayer membranes.[26]

Our theoretical model could add to the understanding of pore energetics as recently investigated by Karatekin et al.[18] For example, these authors measured a dramatic increase of the transient pore lifetime induced by the detergent Tween 20, which has an anisotropic polar headgroup. The importance of the anisotropy of such polar heads of the detergents for the stability of anisotropic membrane structures has been indicated recently. It has been shown that a single-chain detergent with an anisotropic dimeric polar head (dodecyl D-maltoside) may induce tubular nanovesicles[32] in a way similar to those induced by strongly anisotropic dimeric detergents.[31]

Our approach could also add to the understanding of pore formation induced by certain antimicrobial peptides.[8,19] These peptides are often amphipathic, partially penetrating the host membrane. In addition to that, they have a pronounced elongated shape, which arises from their α-helical backbone structure and, apparently, renders them highly anisotropic. Some of these peptides are believed to cooperatively self-assemble into membrane pores. Thus, they not only facilitate pore formation, but they *actively* induce it. Despite their importance, there are currently few theoretical investigations about the energetics of peptide-induced pore formation.[11,12,14,53] Our model provides perhaps the most simple way to capture the underlying physics of peptide-induced pore formation in lipid membranes.

Discussion of Approximations. We analyzed the energetics of a single membrane pore on the basis of a simple, physically transparent model. It involves a number of approximations that we discuss in the following.

We adopted a phenomenological expression for the membrane−inclusion interaction energy. This expression is valid on a mean-field level. The "mean field" is provided by the local membrane curvatures, C_1 and C_2, that adjust to minimize the system's free energy. This approach is, similar to the Helfrich bending energy, valid if the local curvatures, C_1 and C_2, do not change too drastically. On the other hand, the membrane rim provides local curvatures that differ greatly from those of the planar membrane (the latter, in fact, vanish). Hence, formation of a pore in a planar membrane necessarily involves large curvature changes. Yet, as we have seen, the Helfrich bending energy describes the line tension of an inclusion-free membrane; on the same ground, we are confident about the applicability of the inclusion free energy.

The phenomenological expression for the inclusion free energy, F_i, contains four interaction constants (K, $\bar{K}$, H_m, and D_m). Two of them, H_m and D_m, characterize the shape of the anisotropic inclusion. If the lipid bilayer is required to exactly match the angular shape of individual inclusions, then no further interaction constants are needed. In this case, the angular matching appears as a boundary condition for an appropriate differential equation.[35,36,38,54] In our present approach, an ensemble of inclusions interacts (in a mean-field fashion) with a membrane patch of prescribed principal curvatures (the curvatures may afterward be optimized). In this case, there appear two additional interaction constants, K and $\bar{K}$. These constants account for the energy to insert anisotropic inclusions into a bilayer patch of fixed principal curvatures. This process is supposed to locally perturb the two monolayer leaflets of the bilayer. One can thus roughly obtain the interaction constants, K and $\bar{K}$, by estimating the microscopic (short-range) interaction between the perturbed monolayers and the inclusion. To this end, we used membrane elasticity theory,[46] which involves a spatial decay length, $\xi \approx 1$ nm, of the inclusion-induced perturbation. Note that the discreteness of the lipids should not be neglected at these length scales, yet membrane elasticity theory actually does neglect it. Still, this approach is commonly used to estimate membrane−inclusion interactions and, where possible, gives good agreement with experimental observations.[55,56]

There are structural approximations concerning the membrane pore. Its shape is assumed to be circular, covered by a semitoroidal rim. These assumptions seem to us the most reasonable ones. Still, there could be, say, an inclusion-induced change in the cross-sectional shape of the membrane rim. In fact, we performed additional calculations in which we allowed for a semiellipsoidal shape of the membrane rim. The free energy was then minimized with respect to the corresponding aspect ratio. With this additional degree of freedom, we found qualitatively the same results as with the semitoroidal rim.

The statistical mechanical approach to derive the inclusion free energy F_i in eq 13 assumes noninteracting, pointlike particles. Even though we ensured that the number of inclusions in the pore, N_P, never exceeds the sterically possible maximal number, N_P^{max}, we cannot exclude direct inclusion−inclusion interactions within the pore. In fact, such interactions are important in nearly all realistic situations. The average distance between neighboring inclusions in membrane pores is generally

of the order of molecular dimensions. Hence, direct interactions matter. Yet, these interactions are specific, depending on molecular details. Our approach is of generic nature; specific interactions add to the mechanisms specified in our work.

Finally, we employed linearized PB theory. Calculations within nonlinear PB theory with regard to the semitoroidal shape of the membrane rim and the local demixing between charged and uncharged lipids are much more demanding but are currently being carried out.

None of the approximations employed can detract from our principal conclusion: anisotropic membrane inclusions are candidates for the energetic stabilization of membrane pores.

Conclusions

Our theoretical approach adds three aspects to the analysis of pores in lipid membranes. First, the modification of the elastic properties of the membranes in the presence of inclusions is taken into account, as is reflected in the calculation of the membrane−inclusion interaction constants. Second, we allow for anisotropy of the inclusions, which enables us to consider various inclusion shapes, conelike, inverted conelike, wedgelike, and saddle-like inclusions. Third, the lateral density of the inclusions is not kept constant. Instead, we calculate the pore energetics for a fixed chemical potential of the inclusions. The last point is especially important in studies where the admixed compounds are predominantly localized in the region of the pore edges, such as the detergent sodium cholate[18] or the protein talin.[57] Our model is simple and approximate, but it provides a lucid and reproducible framework to analyze pore formation in lipid membranes.

Acknowledgment. We are indebted to A. Ben-Shaul, S. Bezrukov, D. Miklavčič, H. Hägerstrand, and M. Kandušer for stimulating discussions and to MESS of the Republic of Slovenia for financial support. S.M. thanks TMWFK for support.

References and Notes

(1) Lieber, M. R.; Steck, T. L. *J. Biol. Chem.* **1982**, *257*, 1660−1666.
(2) Lieber, M. R.; Steck, T. L. *J. Biol. Chem.* **1982**, *257*, 1651−1659.
(3) Lew, V. L.; Muallem, S.; Seymour, C. A. *Nature* **1982**, *296*, 742−744.
(4) Abidor, I. G.; Arakelyan, V. B.; Chernomordik, L. V.; Chizmadzhev, Y. A.; Pastushenko, V. F.; Tarasevich, M. R. *Bioelectrochem. Bioenerg.* **1979**, *6*, 37−52.
(5) Neumann, E., Sowers, A. E., Jordan, C. A., Eds. *Electroporation and Electrofusion in Cell Biology;* Plenum Press: New York and London, 1989.
(6) Lee, R. C.; Kolodney, M. S. *Plast. Reconstr. Surg.* **1987**, *80*, 663−671.
(7) Wolf, H.; Rols, M. P.; Boldt, E.; Neumann, E.; Teissie, J. *Biophys. J.* **1994**, *66*, 524−531.
(8) Shai, Y. *Biophys. Biochim. Acta* **1999**, *1462*, 55−70.
(9) Crowley, J. M. *Biophys. J.* **1973**, *13*, 711−724.
(10) Isambert, H. *Phys. Rev. Lett.* **1998**, *80*, 3404−3407.
(11) Zemel, A.; Fattal, D. R.; Ben-Shaul, A. *Biophys. J.* **2003**, *84*, 2242−2255.
(12) Zuckermann, M. J.; Heimburg, T. *Biophys. J.* **2001**, *81*, 2458−2472.
(13) Sperotto, M. M. *Eur. Biophys. J.* **1997**, *26*, 405−416.
(14) Lin, J. H.; Baumgaertner, A. *Biophys. J.* **2000**, *78*, 1714−1724.
(15) May, S. *Eur. Phys. J. E* **2000**, *3*, 37−44.
(16) Chernomordik, L. V.; Kozlov, M. M.; Melikyan, G. B.; Abidor, I. G.; Markin, V. S.; Chizmadzhev, Y. A. *Biochim. Biophys. Acta* **1985**, *812*, 643−655.
(17) Litster, J. D. *Phys. Lett.* **1975**, *53*, 193−194.
(18) Karatekin, E.; Sandre, O.; Guitouni, H.; Borghi, N.; Puech, P. H.; Brochard-Wyart, F. *Biophys. J.* **2003**, *84*, 1734−1749.
(19) Huang, H. W. *Biochemistry* **2000**, *39*, 8347−8352.
(20) Nomura, F.; Nagata, M.; Inaba, T.; Hiramatsu, H.; Hotani, H.; Takiguchi, K. *Proc. Natl. Acad. Sci. U.S.A.* **2001**, *98*, 2340−2345.
(21) Betterton, M. D.; Brenner, M. P. *Phys. Rev. Lett.* **1999**, *82*, 1598−1601.
(22) Fournier, J. B. *Phys. Rev. Lett.* **1996**, *76*, 4436−4439.
(23) Kralj-Iglič, V.; Svetina, S.; Žekš, B. *Eur. Biophys. J.* **1996**, *24*, 311−321.
(24) Marčelja, S. *Biophys. Biochim. Acta* **1976**, *455*, 1−7.
(25) Leibler, S.; Andelman, D. *J. Phys. (Paris)* **1987**, *48*, 2013−2018.
(26) Iglič, A.; Kralj-Iglič, V. Effect of anisotropic properties of membrane constituents on membrane bilayer structures. In *Membrane Science and Technology, Vol. 7: Planar Lipid Bilayers (BLMs) and their Applications*; Tien, H. T., Ottova-Leitmannova, A., Eds.; Elsevier: Amsterdam, New York, 2003.
(27) Kralj-Iglič, V.; Heinrich, V.; Svetina, S.; Žekš, B. *Eur. Phys. J. B* **1999**, *10*, 5−8.
(28) Kralj-Iglič, V.; Iglič, A.; Gomišček, G.; Sevšek, F.; Arrigler, V.; Hägerstrand, H. *J. Phys. A: Math. Gen.* **2002**, *35*, 1533−1549.
(29) Chanturiya, A.; Yang, J.; Scaria, P.; Stanek, J.; Frei, J.; Mett, H.; Woodle, M. *Biophys. J.* **2003**, *84*, 1750−1755.
(30) Malev, V. V.; Schagina, L. V.; Gurnev, P. A.; Takemoto, J. Y.; Nestorovich, E. M.; Bezrukov, S. M. *Biophys. J.* **2002**, *82*, 1985−1994.
(31) Kralj-Iglič, V.; Iglič, A.; Hägerstrand, H.; Peterlin, P. *Phys. Rev. E* **2000**, *61*, 4230−4234.
(32) Hägerstrand, H.; Kralj-Iglič, V.; Bobrowska-Hägerstrand, M.; Iglič, A. *Bull. Math. Biol.* **1999**, *61*, 1019−1030.
(33) Gil, T.; Ipsen, J. H.; Mouritsen, O. G.; Sabra, M. C.; Sperotto, M. M.; Zuckermann, M. J. *Biophys. Biochim. Acta* **1998**, *1376*, 245−266.
(34) Goulian, M. *Curr. Opin. Colloid Interface Sci.* **1996**, *1*, 358−361.
(35) Goulian, M.; Bruinsma, R.; Pincus, P. *Europhys. Lett.* **1993**, *22*, 145−150.
(36) Kim, K. S.; Neu, J.; Oster, G. *Biophys. J.* **1998**, *75*, 2274−2291.
(37) Dommersnes, P. G.; Fournier, J. B. *Eur. Phys. J. B* **1999**, *12*, 9−12.
(38) Kim, K. S.; Neu, J.; Oster, G. *Phys. Rev. E* **2000**, *61*, 4281−4285.
(39) Helfrich, W. *Z. Naturforsch.* **1973**, *28*, 693−703.
(40) Taupin, C.; Dvolaitzky, M.; Sauterey, C. *Biochemistry* **1975**, *14*, 4771−4775.
(41) Moroz, J. D.; Nelson, P. *Biophys. J.* **1997**, *72*, 2211−2216.
(42) Andelman, D.; Kozlov, M. M.; Helfrich, W. *Europhys. Lett.* **1994**, *25*, 231−236.
(43) May, S. *Curr. Opin. Colloid Interface Sci.* **2000**, *5*, 244−249.
(44) Verwey, E. J. W.; Overbeek, J. T. G. *Theory of the stability of lyophobic colloids*; Elsevier: New York, 1948.
(45) Andelman, D. Electrostatic properties of membranes: The Poisson−Boltzmann theory. In *Structure and Dynamics of Membranes*, second ed.; Lipowsky, R., Sackmann, E., Eds.; Elsevier: Amsterdam, 1995; Vol. 1.
(46) Dan, N.; Pincus, P.; Safran, S. A. *Langmuir* **1993**, *9*, 2768−2771.
(47) May, S. *Langmuir* **2002**, *18*, 6356−6364.
(48) Dan, N.; Berman, A.; Pincus, P.; Safran, S. A. *J. Phys. II* **1994**, *4*, 1713−1725.
(49) Dan, N.; Safran, S. A. *Biophys. J.* **1998**, *75*, 1410−1414.
(50) Safinya, C. R.; Sirota, E. B.; Roux, D.; Smith, G. S. *Phys. Rev. Lett.* **1989**, *62*, 1134−1137.
(51) Troiano, G. C.; Tung, L.; Sharma, V.; Stebe, K. J. *Biophys. J.* **1998**, *75*, 880−888.
(52) Kandušer, M.; Fošnarič, M.; Šentjurc, M.; Kralj-Iglič, V.; Hägerstrand, H.; Iglič, A.; Miklavčič, D. *Colloids Surf., A* **2003**, *214*, 205−217.
(53) Biggin, P. C.; Sansom, M. S. P. *Biophys. Chem.* **1999**, *76*, 161−183.
(54) Weikl, T. R.; Kozlov, M. M.; Helfrich, W. *Phys. Rev. E* **1998**, *57*, 6988.
(55) Harroun, T. A.; Heller, W. T.; Weiss, T. M.; Yang, L.; Huang, H. W. *Biophys. J.* **1999**, *76*, 3176−3185.
(56) Lundbæk, J. A.; Andersen, O. S. *Biophys. J.* **1999**, *76*, 889−895.
(57) Saitoh, A.; Takiguchi, K.; Tanaka, Y.; Hotani, H. *Proc. Natl. Acad. Sci. U.S.A.* **1998**, *95*, 1026−1031.